NeuroImage 147 (2017) 219–232

Contents lists available at ScienceDirect

NeuroImage

journal homepage: www.elsevier.com/locate/neuroimage

Evaluation of cortical local field potential diffusion in stereotactic electro-encephalography recordings: A glimpse on white matter signal

Manuel R. Mercier [a,b,f], Stephan Bickel [a], Pierre Megevand [c], David M. Groppe [c], Charles E. Schroeder [d,e], Ashesh D. Mehta [c], Fred A. Lado [a,b,*]

[a] Department of Neurology, Montefiore Medical Center, 111 East 210th Street, Bronx, NY 10467, USA
[b] Department of Neuroscience, Albert Einstein College of Medicine, 1410 Pelham Parkway South, Bronx, NY 10461, USA
[c] Department of Neurosurgery, Hofstra-Northwell School of Medicine and Feinstein Institute for Medical Research, Manhasset, New York, NY 11030, USA
[d] Cognitive Neuroscience and Schizophrenia Program, Nathan Kline Institute, Orangeburg, NY 10962, USA
[e] Department of Neurosurgery, Columbia College of Physicians and Surgeons, New York, NY 10032, USA
[f] Centre de Recherche Cerveau et Cognition (CerCo), CNRS, UMR5549, Pavillon Baudot CHU Purpan, BP 25202, 31052 Toulouse Cedex, France

ARTICLE INFO

Article history:
Received 26 August 2015
Accepted 18 August 2016
Available online 21 August 2016

Keywords:
Epilepsy
Stereotactic electroencephalography
White matter
Gray matter
Intracranial reference
Brain state

ABSTRACT

While there is a strong interest in meso-scale field potential recording using intracranial electro-encephalography with penetrating depth electrodes (i.e. stereotactic EEG or S-EEG) in humans, the signal recorded in the white matter remains ignored. White matter is generally considered electrically neutral and often included in the reference montage. Moreover, re-referencing electrophysiological data is a critical preprocessing choice that could drastically impact signal content and consequently the results of any given analysis. In the present stereotactic electroencephalography study, we first illustrate empirically the consequences of commonly used references (subdermal, white matter, global average, local montage) on inter-electrode signal correlation. Since most of these reference montages incorporate white matter signal, we next consider the difference between signals recorded in cortical gray matter and white matter. Our results reveal that electrode contacts located in the white matter record a mixture of activity, with part arising from the volume conduction (zero time delay) of activity from nearby gray matter. Furthermore, our analysis shows that white matter signal may be correlated with distant gray matter signal. While residual passive electrical spread from nearby matter may account for this relationship, our results suggest the possibility that this long distance correlation arises from the white matter fiber tracts themselves (i.e. activity from distant gray matter traveling along axonal fibers with time lag larger than zero); yet definitive conclusions about the origin of the white matter signal would require further experimental substantiation. By characterizing the properties of signals recorded in white matter and in gray matter, this study illustrates the importance of including anatomical prior knowledge when analyzing S-EEG data.

1. Introduction

The surgical treatment of pharmacoresistant epilepsy most often requires placement of intracranial electrodes to determine the cortical zones responsible for seizures and to identify regions of eloquent cortex. While locations targeted for electrode placement are selected by clinicians based on the suspected zone(s) of seizure onset, researchers also make use of these electrodes to study electrical activity recorded directly from the human brain. These recordings are made either using subdural grids and strips to record the electrocorticogram (ECoG) (Penfield and Steelman, 1947) or penetrating stereotactic electroencephalography (S-EEG) electrodes that record from contacts along the length of the electrode shaft (Bancaud and Talairach, 1973; Spiegel et al., 1947; Talairach et al., 1974; Talairach and Szikla, 1980). The latter method permits targeting deep or remote cortical regions and, as a consequence, some of the recording contacts on the electrode shaft are located in the white matter.

As with any electrical recording, intracranial electro-encephalographic recordings (iEEG) require the use of a reference that ideally should be has *neutral* as possible to avoid any spurious contamination. In reality, however, single or multiple contacts used as the “reference” add signal to the recording. Some common references, such as a scalp electrode or average reference, blend signal from multiple brain regions, whereas “local” references, like bipolar or Laplacian montages, reference recorded signals to

* Corresponding author at: Department of Neurology, Montefiore Medical Center, 111 East 210th Street, Suite H-020, Bronx, NY 10467, USA
E-mail address: flado@montefiore.org (F.A. Lado).

http://dx.doi.org/10.1016/j.neuroimage.2016.08.037
1053-8119/

neighboring electrode contacts (Bastos and Schoffelen, 2015; Boatman-Reich et al., 2010; Lachaux et al., 2003). When S-EEG electrodes are used, contacts may be located in non-gray matter tissues, such as white matter. Consequently, signal from non-gray matter contacts are combined with iEEG signal when an average or local reference is used (Zaveri et al., 2006). Little is known, however, about the electrophysiological properties of white matter, and consequently, about the relative contribution to intracranial recordings of electrical activity from white matter. The blending of gray and white matter signals in the reference may be a crucial issue since field potentials comprising the iEEG are typically ascribed to synaptically induced current flow in neurons located in gray matter; whereas the source of electrical activity in white matter is current flow through voltage-gated channels mediating action potentials in axons connecting widely separated neuronal populations. Therefore, gray matter and white matter contain electrical activity reflecting, respectively, spatially circumscribed cortical activity and the distributed communication between cortical nodes of large scale networks. Moreover, gray and white matter present different characteristics regarding volume conduction: while field potential signal passively spreads laterally as well as vertically in gray matter, in white matter the denser myelin sheaths may asymmetrically constrain current flow and signal propagation (Kajikawa and Schroeder, 2011, 2015).

In the present study, we describe the influence that the choice of reference has on the signal properties of intracranial data, and we investigate the differences between signals recorded in the gray and white matter. Based on a new method of electrode contact classification that takes into account the tissue surrounding recording contacts, our analyses reveal that signals emanating from gray matter are larger in magnitude and tend to spread by volume conduction into nearby white matter. We show as well that appropriate referencing can isolate white matter signal, which may reflect massed firing in fibers of passage, whose cell bodies lie elsewhere. These results highlight the biases intrinsic in the use of recording reference and the importance of not discounting the signal activity recorded in white matter when analyzing human intracranial data.

2. Materials and methods

2.1. Participants

Data were collected from 7 patients (4 males, mean ± s.d. age: 29.3 ± 10.5 yrs, 7 right handed) implanted stereotactically with depth electrodes in the course of their evaluation for epilepsy surgery. One patient was also implanted with a subdural electrode grid and electrode strips (these electrode contacts were not used in the main analysis). Participants provided written informed consent, and the Institutional Review Boards of Montefiore Medical Center and Hofstra North Shore-LIJ approved the procedures. The study conformed to the principles outlined in the Declaration of Helsinki.

2.2. Electrode localization

In total, 1082 electrode contacts were implanted (mean ± s.d. 147 ± 57 per patient), their number and placement were determined solely by medical needs. Depth electrode diameter was 1.1 mm, and each contact was 2.4 mm in length, and inter-contact spacing was 5 mm; for subdural grid and strip electrodes, contact diameter was 5 mm with 2.3 mm exposure and 10 mm between electrode contacts (ADtech, Racine, WI; Integra Life-sciences, Plainsboro, NJ). To precisely localize electrode contacts, the location of each contact centroid was first manually identified on a post-implant CT scan using Bioimage Suite (X. Papademetris, M. Jackowski, N. Rajeevan, H. Okuda, R.T. Constable, and L.H Staib. BioImage Suite: an integrated medical image analysis suite, Section of Bioimaging Sciences, Dept. of Diagnostic Radiology, Yale School of Medicine). The locations were then mapped to the pre-implant MRI brain via a rigid affine transformation using FLIRT (Jenkinson and Smith, 2001), that was derived from co-registration of post-implant CT scan to post-implant MRI and of post-implant MRI to pre-implant MRI. Both co-registration procedures were performed with the Oxford Centre for Functional MRI of the Brain (FMRIB) software library (FSL: www.fmrib.ox.ac.uk/fsl). For the one patient that was also implanted with a subdural grid and strips, electrode contact coordinates were projected to the smoothed pial surface of the pre-implant MRI (a simplified version of the algorithm presented in (Dykstra et al., 2012)). The pial surface was reconstructed from the pre-implant MRI using FreeSurfer (http://surfer.nmr.mgh.harvard.edu/). Cortical and subcortical brain regions were parcellated using Freesurfer (Fischl et al., 2004) and brain regions were labeled using the Destrieux atlas (Destrieux et al., 2010). For identical intracranial electrode localization methods see (Groppe et al., 2013; Keller et al., 2013, 2014). This method is now freely available in the iELVis open source toolbox (http://biorxiv.org/content/early/2016/08/11/069179), and is extensively described on the toolbox wiki (http://episurg.pbworks.com). The toolbox can be downloaded from https://github.com/episurg/EpiSurg.

S-EEG electrode contacts were then classified using a gradual approach reflecting the composition of tissue surrounding the contact centroid. That is, based on identified regions from the Freesurfer parcellation, the proportion of cortical gray and white matter MRI voxels contiguous to the centroid of each contact was estimated. The tissue mix surrounding each electrode contact was defined using the index of proximal tissue density (PTD) as follows:

$$PTD=(VoxGray–VoxWhite)/(VoxGray + VoxWhite)$$

where VoxGray and VoxWhite are the number of gray and white matter voxels, respectively, in a 3x3x3 mm^3 volume surrounding the centroid of the electrode contact (i.e., 26 voxels). The size of PTD sample volume was based on the magnitude of the approximations inherent in localizing electrode contacts, such as imaging voxel resolution of 1 mm^3, estimated co-registration errors, and electrode contact size (see Fig. 1A for a schematic illustration). The PTD measure can easily be adapted to higher image resolution by increasing the size of the number of voxels surrounding the centroid used to compute the PTD.

This “fuzzy” approach applying a gradual gray-white classification of contacts was used for two reasons: (1) cortically generated voltages spread passively, so that an electrode contact may record activity that did not originate in the immediate vicinity of the electrode; (2) to reflect a degree of uncertainty in the location of the electrode contacts. Regarding the latter issue, there are several factors that limit our ability to precisely localize electrode contacts. First the centroid of the artifact might not be the center of mass of the electrode contact because of the orientation of the electrode shaft with respect with the CT image slices. Second, the co-registration procedure for aligning CT and MRI images may introduce affine deformations that could slightly shift the location of an electrode contact (several mm depending on MR resolution). Third, the gray-white matter parcellation procedure includes spatial smoothing that could affect the classification of electrode contacts located near a gray-white junction. Uncertainty in the localization and co-registration to MRI of implanted electrode contacts is not specific for any one method and has been discussed in the literature (Dalal et al., 2008; Hermes et al., 2010; Ken et al.,

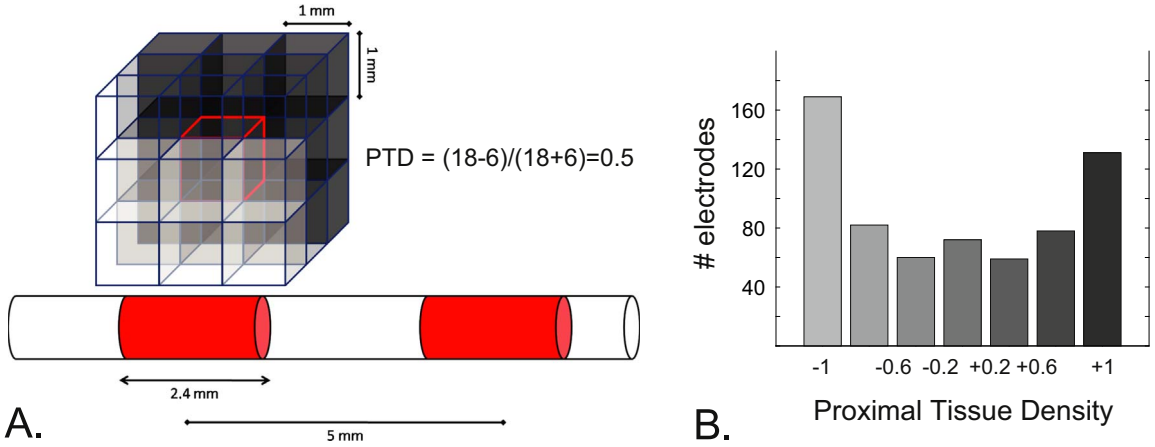

Fig. 1. Illustration of the Proximal Tissue Density index (PTD), **A.** Schematic drawing comparing size and geometry of stereotaxic electrode and MRI voxels. Each cube in the larger volume represents one voxel. Voxels may contain cortical gray matter (in black, e.g. $n=18$), white matter (white transparent, e.g. $n=6$), or neither cortical gray matter nor white matter (transparent, e.g. $n=3$). Stereotaxic electrode contacts measure 2.4 mm in length and span multiple voxels. **B.** Aggregate histogram illustrating total number of electrode contacts from all patients found in eachPTD range (white matter only: -1; -1 to -0.6; -0.6 to $-.02$; -0.2 to $+0.2$; $+0.2$ to $+0.6$; and gray matter only: $+1$).

2007; LaViolette et al., 2011; Miller et al., 2007; Sebastiano et al., 2006).

The "fuzzy" classification method proposed in the present study differs from a binary classification based on only the location of the centroid of the electrode contact. For the electrode contacts with their centroid located in gray matter ($n=302$), only 42% were entirely surrounded by gray matter (i.e. PTD=1). For electrode contacts with their centroid located in white matter ($n=316$), 43% – nearly the same proportion as for gray matter – were entirely surrounded by white matter (i.e. PTD$=-1$). Approximately 60% of all electrode contacts were surrounded by both white and gray matter (i.e.: $-1<\mathrm{PTD}<1$; see Fig. 1B). Interestingly, a slightly larger number of electrode contacts were located entirely in the white matter than in the gray matter. Note that PTD was computed only for the electrode contacts that had their centroids located in cortical gray or white matter region identified during the parcellation procedure, electrode contacts in other structures were not considered (e.g. hippocampus or amygdala). The rationale for not including non-cortical gray matter electrode contacts in the present study was based on preliminary analysis clearly showing distinct characteristics of the corresponding signal, notably in the power spectral density profile and absolute amplitude modulation during the three states.

2.3. Intracranial EEG recording and preprocessing

Patients were recorded continuously at Montefiore Medical Center (Bronx, NY) and at North Shore LIJ (Nassau, NY) using clinical EEG-CCTV systems (Natus Medical Incorporated, San Carlos, CA, USA). Data were sampled at either 500 Hz or 512 Hz. CCTV video was reviewed off-line and annotated with regard to patient activity. In the present study 3 states of activity were selected: (i) nocturnal sleep at times the patient was immobile and iEEG showed intermittent slow delta oscillations indicative of deep sleep (stage N3, formerly stages 3 and 4); (ii) daytime wakefulness while watching video entertainment on television or computer and while lying immobile in bed, and (iii) daytime wakefulness while involved in active conversation, which included listening, speaking and making gestures. The goal of the present report is not to study differences between the different patient states of activity, but rather to demonstrate that electrophysiological features characterizing gray and white matter are independent of 'brain states'.

For each patient, a 5 to 10 min data period, corresponding to each of the three states of activity, was extracted and used for analysis. Continuous data were visually inspected to reject periods containing artifacts and to reject noisy electrode contacts from all analysis and reference montage. Selected data was then segmented into 3 s non-overlapping epochs. The mean $\pm$ s.d. number of epoch across participants was 97 ± 26 for "sleep" data, 76 ± 14 for "passive watching" data and 88 ± 11 for "active discussion" data. Epochs were detrended, demeaned and notch filter was applied to remove line noise and harmonics (60, 120, 180 and 240 Hz).

2.4. Reference montages

Data were recorded using a subdermal electrode placed in the parieto-frontal regions of the skull as a recording reference (Vulliemoz et al., 2010). To investigate the influence of the reference montage used on signal content, we additionally re-referenced the signal using four approaches: a white matter average reference, a gray matter average reference, a global average reference; and a local reference montage. For the white (gray) matter average reference montage, the signals of all artifact-free electrode contacts with a PTD of -1 (PTD$+1$) were averaged and subtracted from the signal recorded at each electrode contact. For the average reference montage, all artifact-free electrode contacts were used regardless of their anatomical location. For the local reference, a composite scheme using the nearest electrode contact neighbors was applied to estimate the local field potential second spatial derivative (i.e. the Laplacian), using Eq. (1) for 1 dimension implants (depth and strip electrode contacts) and Eq. (2) for two dimensional implants (grid).

$$(V_k)' = V_k - 1/2 \times (V_{k+1} + V_{k-1}) \quad (1)$$

$$(V_{i,j})' = V_{i,j} - 1/4 \times (V_{i+1,j} + V_{i-1,j} + V_{i,j+1} + V_{i,j-1}) \quad (2)$$

where V_k (or $V_{i,j}$) is the recorded field potential at the kth position (or at the ith row and jth column) in the electrode depth shaft or strip (or grid) and $(V_k)'$ (or $(V_{i,j})'$) is the signal re-referenced to a local reference. The number of neighboring electrode contacts used varied from 1 to 4 on the basis of the montage (depth, strip or grid), on the location of the electrode contact in the montage (periphery or center), and on the quality of the electrical signal (i.e., only artifact-free electrode contacts were used). This

approach was used to ensure maximum representation of the reliable local signals available (see for identical approach: (Butler et al., 2011; Gomez-Ramirez et al., 2011; Mercier et al., 2013, 2015; Shirhatti et al., 2016)).

The second spatial derivative used here for depth, strip and grid electrode recordings is similar to the current source density approach used in surface EEG which also computes the second spatial derivative to estimate current sources (Hjorth, 1975; Perrin et al., 1987; Shepard, 1968).

2.5. Signal analysis and testing

2.5.1. Reference montage and signal correlation analysis

The influence of the reference montage on signal magnitude correlation calculated between all pairs of electrode contacts was computed using Pearson correlation coefficient, for each epoch and then averaged over all epochs. Also, to evaluate the influence of the reference on signal correlation across all participants, absolute correlation measures were averaged for all depth electrode contacts across patients for each reference montage. Only data recorded with stereo-EEG electrodes were used in the case of the patient that also had subdural electrode strips and grids.

2.5.2. Gray/white matter signal characterization

To investigate if there are differences between signals recorded from cortical gray matter and white matter, the signal recorded from depth electrode contacts were grouped based on their surrounding tissue type. Following the gradual tissue classification scheme, 7 bins were defined using the PTD index (Fig. 1B): white matter only (PTD$=-1$), from -1 to -0.6, -0.6 to -0.2, -0.2 to $+0.2$, $+0.2$ to $+0.6$, $+0.6$ to $+1$ and gray matter only (PTD$=+1$). To minimize signal contamination by the reference, analyses were performed on data first using the global average reference and again using a local reference.

In characterizing the differences between gray and white matter signal, we first compared the spectral properties of each signal. The spectral profile of the signal recorded from each electrode contact was computed using a Fast Fourier transform of each epoch after application of a Hanning taper (from 1 to 250 Hz, with a frequency resolution of 1 Hz) and mean power spectra were computed across trials. We next calculated the mean spectral profile for each PTD bin of electrode contacts. To test for statistically significant differences between the two extremes (i.e. PTD$=-1$ and $+1$), an unpaired randomization procedure was applied as follows: each electrode contact was randomly re-classified as belonging to either bin while keeping bin size constant (i.e. each bin contains a random assortment of $+1$ and -1 PTD values). Then the difference between the two random PTD groups was computed. This process was repeated 1000 times to build a surrogate distribution of mean differences that was used to define significance thresholds at each spectral frequency (two tails: 2.5–97.5%). The actual observed differences in the mean spectral power of gray and white matter electrode contacts were determined to be significant if it exceeded the threshold. All p-values were corrected for multiple comparisons along the frequency dimension using the False Discovery Rate procedure from Benjamini & Yekutieli (2001), with the false discovery rate, q-value, set at 5%. This correction, a sequential Bonferroni-type procedure, provides a good tradeoff between Type I and Type II errors of all the conventional techniques available for multiple comparison correction (see (Groppe et al., 2011a, 2011b) for details and empirical simulation).

Next we investigated whether signal amplitude depended on the composition of the surrounding tissue. Note that since trial mean amplitude was equal to zero (due to baseline correction), the mean absolute signal amplitude was used, which is equivalent to the square root of the time dependent variance, a measure of signal fluctuation. For each electrode, mean absolute signal amplitude was computed for each epoch, averaged across epochs, and the mean absolute signal amplitude was computed across electrode contacts grouped according to the seven PTD bins. The relation between the mean absolute amplitude across bins was tested using Spearman correlation and unpaired randomization statistic was applied to test for significant difference between the bins at both extremes of the PTD scale (see description above). The same Benjamini & Yekutieli (2001) procedure, that is guaranteed to be accurate for any test dependency structure, was used to control for multiple comparisons due to the different bins (q-value set at 5%).

2.5.3. Volume conduction of gray matter signal into white matter

Absolute signal amplitude was next used to evaluate the extent to which the signal recorded from white matter is contaminated by passive signal spread from nearby gray matter. To do so, we sorted, binned and averaged the absolute signal amplitude recorded from electrode contacts entirely in the white matter (i.e. PTD$=-1$, $n=168$) based on the distance of each contact to the nearest gray matter. We then calculated the Pearson correlation between the mean absolute amplitude values for each bin and corresponding distances to gray matter. This was done for data referenced to a global average and to the local montage. We applied a similar approach to bipolar white matter signal, that is for adjacent pairs of contacts on the same electrode shaft where both were located in white matter (PTD$=-1$, $n=77$) we subtracted the signal of one on the other – so as to reject signals of distant origin and to focus on local white matter signal. In that case the smallest distance to gray matter of the two electrode contacts of the pair was retained for the binning.

To further assess if the relation between absolute signal amplitude and distance to gray matter reflect passive signal spread rather than generation of voltage from local activity, the same analysis was conducted a second time, on all data sets, with the distance to gray matter transformed to the inverse of the square distance (i.e. the strength of an electrical field falls off non-linearly with distance (Kutas and Dale, 1997).

The influence of passive signal spread was further investigated for the different frequencies by applying the same approach based on white matter electrode contacts (PTD$=-1$) binned by their distance to gray matter. This analysis was done using the signal re-referenced to the average and the local montage, subjected to the frequency transform described above (see Section 2.5.2). Power spectra density (PSD) was computed for all white matter contacts located at a given distance to gray matter (bins). To focus on the relative difference between bins, corresponding PSD were normalized using the mean PSD across PSD bin means. That is by subtracting and then dividing each PSD bin by the mean PSD across bins.

2.5.4. Correlation of activity between gray and white matter

To investigate if the signal recorded locally in the white matter actually originated in distant cortical neuronal populations, we next analyzed bipolar signals from pairs of adjacent contacts co-located on the same electrode shaft with either both contacts in white matter or both contacts in gray matter (PTD$=-1$ for white matter electrode-pairs, $n=77$; PTD$=+1$ for gray matter electrode-pairs, $n=24$, 25 and 27 respectively for 'passive watching', 'sleep' and 'active discussion' dataset). As before, we used this bipolar montage to minimize common signal and focus instead on local activity (Bastos and Schoffelen, 2015). Next we calculated the Pearson correlation between bipolar signals from white matter electrode-pairs with the signals from each of the gray matter electrode-pairs. For every white-gray combination, a correlation coefficient was computed for each epoch and then averaged across

trials. Statistical significance was tested using a randomization procedure where the temporal link between the two signals was broken. That is, trials were randomly shuffled before computing the correlation coefficient. This procedure was repeated 1000 times to build a surrogate distribution, from which significant threshold was computed and compared to the observed correlation coefficient. *P*-values from each white-gray matter comparison pair were finally corrected for multiple comparisons using the False Discovery Rate procedure from Benjamini & Yekutieli (2001) with a q-value set at 5%.

In order to consider the possibility that significant correlations between distant gray matter contacts and local white matter electrode contacts arose from passive spread of activity from local adjacent gray matter, we performed an additional series of analysis for each pair of white-gray matter signals. The gray matter electrode contact (as defined by the location of its centroid, see Section 2.2) located closest to the two white matter electrode contacts, was selected and its signal referenced locally (see Section 2.4). This proximal gray matter local signal was then correlated (Pearson correlation) for each trial with signal from the nearby white matter and the signal from distant gray matter. Next, the resulting correlation coefficients (*r*-values of each trial) were correlated to obtain an estimate of the link between local correlation (i.e. between white matter and proximal gray matter) and distant correlation (i.e. between distant gray matter and proximal gray matter). The obtained *p*-value indicated if the signals from the white and the distant gray matter were significantly correlated due to a common gray matter source located in the gray matter near the white matter.

A last series of analysis were conducted to evaluate how time delay may distinguish passive spread from possible neuronal conduction (or other possible mechanisms causing long range correlation). This was assessed using cross-correlation lags between signals. That is, cross-correlations were computed on single trials (with lag range set between +/− 100 ms), then lags corresponding to the maximal absolute correlation were averaged across trials. Absolute lags distribution obtained for the two populations of electrode contacts of interest (see below) were next compared using a two-sample Kolmogorov–Smirnov to test if the two distributions were identical or not. First, cross-correlation was computed between white matter and proximal gray matter signals either referenced to a global average montage (for electrode contacts pairs located in the white matter the mean signal of the two was used) or to a bipolar local montage (same as in the correlation analysis described in the previous paragraph). Our hypothesis being that the average reference montage should lead to a narrower absolute distribution due to additional zero lag cross-correlation caused by passive spread (i.e. reduced when the bipolar

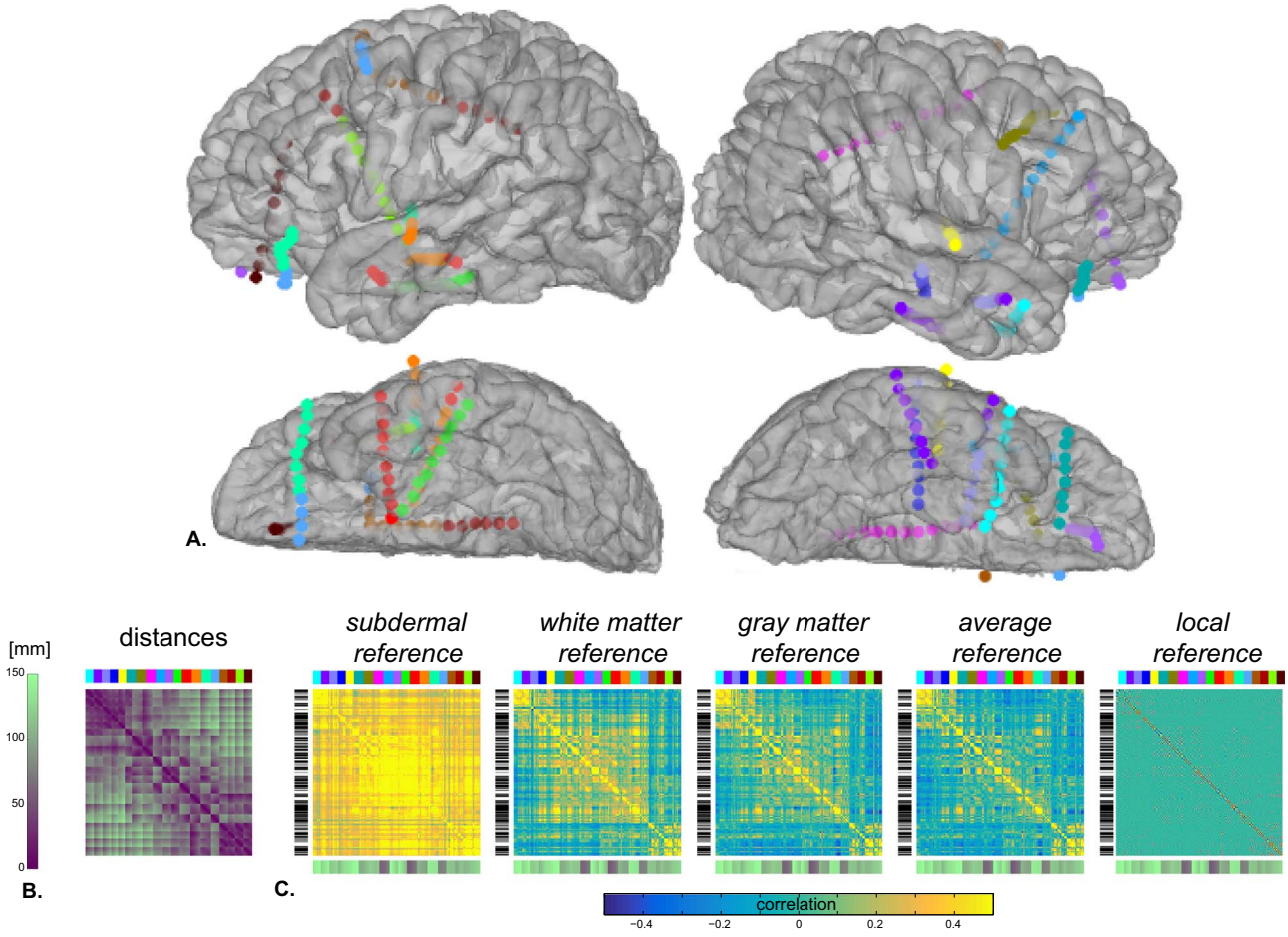

Fig. 2. Example of the influence of reference montage on electrode contacts correlation, Example for one patient: **A.** Depth electrodes localization on patient's surface rendered brain (upper left: left hemisphere lateral view, lower left: left hemisphere ventral view, upper right: right hemisphere lateral view, lower right: right hemisphere ventral view). Each electrode shaft is colored distinctly; the color code is used to identify electrodes in the correlation matrices. **B.** Distances between electrodes in millimeters. The color code above the matrices correspond to the electrode color code used in A. **C.** Correlation matrices between all electrodes with different references (from left to right): subdermal wire (used for recording), white matter average calculated from all electrodes with PTD = −1 ($n_{electrodes}$ = 25), gray matter average calculated from all electrodes with PTD = −1 ($n_{electrodes}$ = 35), average reference from all electrodes ($n_{electrodes}$ = 187) and local reference. The gray level bar code on the left of the matrices represents the Gray-White matter index (from white: PTD = −1 ; to black:, PTD = 1). The color patches above the matrix corresponds to the electrode color code from A. The color code below the matrix represents the distance to the subdermal electrode used to reference the signal during the recording. Data correspond to the 'passive watching' state.

local montage was used) and/or the presence of shared reference signal. Second, we took that same lag distribution corresponding to correlation between proximal gray matter signal and bipolar white matter signal, and compared it to two other lag distributions: from cross-correlation between bipolar white matter signal and distant bipolar gray matter signal, and from cross-correlation between local gray matter and distant bipolar gray matter signal. Here we wanted to evaluate if cross-correlation lag distribution differed depending on the distance between cross-correlated signals.

3. Results

3.1. Influence of the reference on signal correlation

Our first analysis assessed the impact of the reference on intracranial signals by comparing the correlation between electrode contacts with different reference montages. Two examples of this analysis are illustrated: for a patient implanted with depth electrodes only (Fig. 2 for 'passive watching' state and Supplementary Fig 1 for 'sleep' and 'active discussion' state) and for a patient implanted with depth, subdural grid and strip electrodes (Supplementary Fig 2). In both examples, we saw strong correlation values when the data were referenced to a subdermal reference (i.e. used for the recording). This was also the case for signals referenced to the white matter average, or the gray matter average, with stronger overall correlations when the number of white matter electrode contacts used in the average was small (see in Supplementary Fig 2 where there were only 7 white matter electrode contacts in the average, while for the gray matter it was 4). The pattern of correlations between signals referenced to the average resembles the pattern obtained with a subdermal reference and with a white matter average reference reflecting the spatial organization of the electrodes, but the magnitude of the correlation was substantially lower and centered at zero (implying additional negative correlations). The correlation matrices for the local reference montage data, on the other hand, showed a different pattern where correlation between electrode contacts was both sparser and of weaker magnitude.

The observations made in individual cases were confirmed in the larger population (see Fig. 3 and Supplementary Fig. 3), where the mean magnitude correlation across all electrode contacts and patients, showed a correlation reduced by half between subdermal and average reference and by a factor of 6 with a local reference. For white matter average reference only a slight reduction of correlation was observed, and cannot only be explain by a smaller number of electrode contacts since this number of contacts was comparable to the amount used for the gray matter reference. For both average and local reference montage, the smaller standard errors reflected sparse correlation over all electrode contacts. In summary these results showed that the use of either an average or a local reference montage removed the global strong positive correlation (common signal) introduced by the subdermal reference. However, when considering all S-EEG electrode contacts, both the average and local references include signals from multiple tissue types. So far, no systematic investigation has ever been conducted to examine the differences in signals recorded by electrode contacts in white and gray matter. To explore in detail the origin of the signal recorded in these different tissues, we applied a gradual Gray-White matter classification to the electrode contacts and further inquired how the influence of volume conduction can be reduced by different montage references.

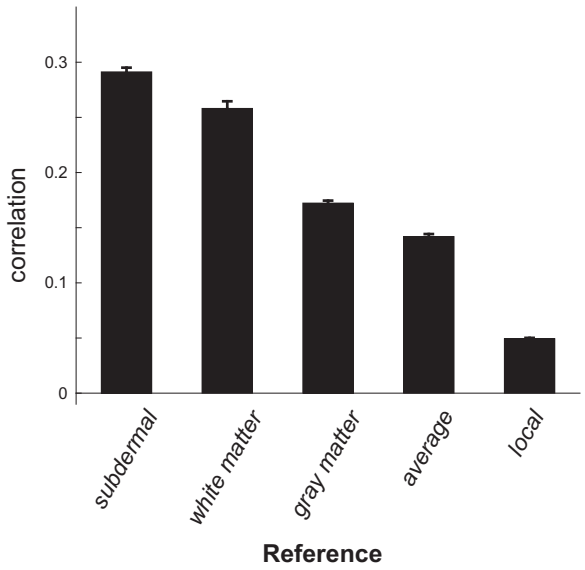

Fig. 3. Influence of reference montage on electrodes correlation, Mean magnitude correlation values across electrodes averaged across patients (± SE, $n=7$) for each reference montage tested. Data correspond to the 'passive watching' state.

3.2. Signal differences between gray and white matter

To investigate the electrophysiological characteristics of the signal recorded from cortical gray and white matter, we analyzed the spectral content of these signals as a function of the surrounding tissue composition. Fig. 4 shows the signal power spectra for electrode contacts grouped by their Proximal Tissue Density value, from white matter only (PTD$=-1$) to gray matter only (PTD$=+1$), for the 'passive watching' data (see also Supplementary Fig. 4 for 'sleep' and 'active discussion' states). Although clearest for the local reference data, both local and average referenced data showed a gradual increase in power at all frequencies with increasing PTD. Additionally, there was a statistically significant difference in power between the two PTD extremes (PTD$=-1$ and $+1$), confirming that activity from contacts in gray matter record greater power. The depiction of the difference between the two extreme PTD spectra (red lines in Fig. 4 and Supplementary Fig. 4) further show that the difference is not random but rather follows the peaks of the main frequency bands (delta, theta, beta and gamma). Next we analyzed signal absolute amplitude to determine whether signal differed systematically between tissues. Using the same grouping approach as for power spectra, absolute amplitude from each contact was binned according to the PTD index, with results shown in Fig. 4, parts C and D (see also Supplementary Fig. 4 for 'sleep' and 'active discussion' states). Correlation analysis conducted on the groups of electrode contacts binned by PTD index reveals a monotone statistical relationship between PTD value and absolute amplitude (Spearman correlation respectively for average and local reference montage; 'passive watching': $r=0.75$; $p<0.07$ and $r=0.96$; $p<0.003$, 'sleep': $r=0.85$; $p<0.02$ and $r=0.96$; $p<0.003$; 'active discussion': $r=0.86$; $p<0.03$ and $r=0.96$; $p<0.003$). Mean absolute signal amplitude was significantly larger at gray matter electrode contacts compared to white matter contacts. (PTD$=+1$ and -1, respectively; unpaired statistics were at $p<0.001$ for both average and local references and for all behavioral states). Again, the analysis of locally referenced measures of absolute amplitude better distinguished the signals arising from white and gray matter. The same analysis were performed on signal variance (computed along time dimension) and led to identical results.

In summary, this analysis confirmed that power spectra and absolute amplitude of spontaneous activity differed significantly between the gray matter and the white matter; and that on

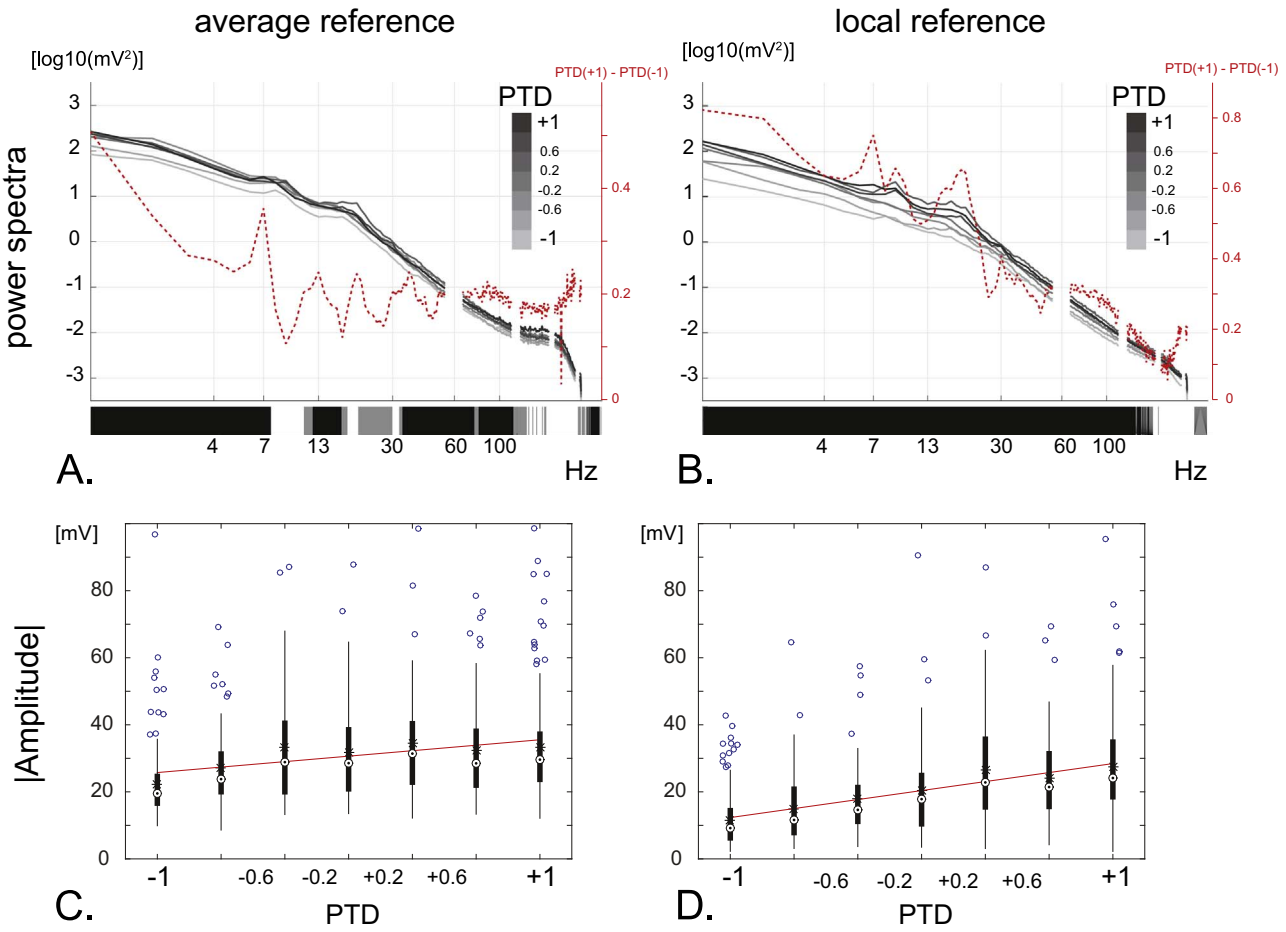

Fig. 4. Gray-White matter signal characteristics, Power spectral density (**A** and **B**) and absolute amplitude (**C** and **D**) vary gradually with the tissue composition (PTD) surrounding the electrodes: from gray matter only (dark gray, PTD = 1) to only white matter (light gray, PTD = −1). In **A.** and **C.** results were obtained with average reference montage, in **B.** and **D.** with a local reference montage. **A.** and **B.** depict power spectra data represented with a logarithmic scale, values for 60 Hz ±5 and harmonics are not shown. The red dashed line represents the difference between the extreme PTD values (−1 and +1); scale is represented on the right *y*-axis in red. Ribbon plot along the *x*-axis represents the results of statistical comparison with corrected significant *p*-values plotted in black and uncorrected *p*-values in gray. **C.** and **D.** depict signal mean absolute amplitude with box plot (mean and median represented by stars and circles respectively), the edges of each boxes represent to the 25th and 75th corresponding percentiles the whiskers extend to the most extreme data points not considered outliers (< 2.7 sigma ; 99.3 data coverage). Outliers are depicted in blue. Red line represents the least-squares fit for all data. Data correspond to the 'passive watching' state.

average the largest signal power and absolute amplitude (and signal fluctuations) were found in the gray matter. Furthermore, we noted that the use of a local reference tended to better separate white and gray matter signals by emphasizing local activity.

3.3. *Influence of local passive spread of activity*

Since absolute signal amplitude was larger in gray matter than in white matter, we hypothesized that the signal recorded by electrode contacts located in the white matter was contaminated by passive signal spread from nearby gray matter. We tested this hypothesis by measuring how the mean absolute signal amplitude from white matter electrode contacts varied with the distance to the nearest gray matter. The results, depicted in Fig. 5 part A (see the black line as well as Supplementary Fig. 5 part A and C for 'sleep' and 'active discussion' states), revealed a negative correlation between absolute signal amplitude and the distance to gray matter (with $r < -0.55$ for all states). Next, we assessed if the observed mean absolute amplitude declined with increasing distance to gray matter, was due to volume conduction effect. To do so, we performed the same analysis with the data transformed to reflect the decline of the voltage with distance, assuming that the signal was originated in the near gray matter. As depicted in Fig. 5 part B (and Supplementary Fig. 5 part B and D), the absolute amplitude decay was more strongly correlated ($r \leq -0.68$ for all states) when the data were modeled as the inverse of the squared distance. Still, the curved shape of the line suggests that the resistance is not perfectly isotropic and indicates that other factors might influence the passive spread, such as the presence of myelin fiber. Interestingly, both analyses revealed that the influence of passively propagated gray matter signal plateaued after 4–5 mm, indicating that beyond this distance the magnitude of the propagated signal was smaller than the magnitude of local activity.

To verify that passive spread of signal from gray matter was responsible for this effect, we re-referenced the white matter signal using a local and a bipolar montage; with the latter only comprised of adjacent contact pairs along the same electrode shaft where both electrode contacts in the pair were fully located in the white matter (PTD = −1). The results, represented respectively by the purple and the orange line in Fig. 5 part A (and Supplementary Fig 5 part A and C), did not show the previously observed decrease in mean absolute signal amplitude with increasing distance to gray matter. This was also the case when the data were modeled non-linearly to take into account volume conduction effects (Fig. 5B and Supplementary Fig. 5B and D).

To characterize how the reference influences passive signal spread at each frequency the same analysis was performed on the frequency spectra, with the signal referenced to the average and

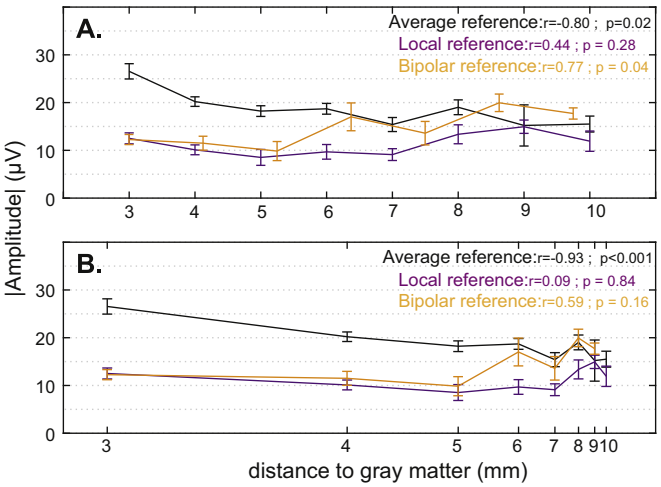

Fig. 5. Evaluation of passive signal spread from gray to white matter, Absolute signal amplitude in the white matter diminishes as a function of the distance to gray matter when data are referenced to an average reference (black) but not when referenced to a local (purple) or bipolar montage reference (orange) indicating that passively spread voltage from gray matter can be recorded millimeters away. Each data point corresponds to the mean variance (+/− SE) for electrodes located in the white matter (PTD=-1)located at a given distance from the gray matter (in voxel/mm). The data are represented and tested (Pearson correlation) on a linear scale in **A** and modeled as 1/distance^2 in **B**. Data correspond to the 'passive watching' state.

the local montage. The results, are illustrated in Fig. 6 (and Supplementary Fig. 6 for 'sleep' and 'active discussion' states), by representing the relative PSD difference of the mean spectra profile of signals from the white matter electrode contacts (PTD$=-1$), binned by their distance to gray matter. Relative PSD difference was computed using the mean PSD across mean PSD bins. For the average reference, as distance to gray matter increases, signal power strongly decreased in the high frequencies (gamma band) with a plateau at about 6mm. For the local reference montage, the same fall off was observed at smaller distances from gray matter, illustrating the effect of local reference on passive signal spread: signal is spatially more focused. Interestingly, when the local reference montage was used, the relative amount of power diminished first to rise again for the larger distances, suggesting that some broad band signal power in the white matter is not due to passive spread of activity from gray matter.

Taken together, these results confirmed the benefit of the local and the bipolar reference montages in isolating local signals by reducing passive spread from surrounding regions. Furthermore, our results indicated that electrode contacts located in the white matter recorded a mix of passively spread higher amplitude activity from nearby gray matter combined with a local signal of smaller amplitude.

3.4. Correlation between white matter signal and gray matter activity

As a final analysis we investigated if the isolated signal recorded in the white matter was correlated with activity recorded elsewhere in the gray matter. That is, for each patient, we computed the zero-lag correlation between each white matter bipolar signal and each gray matter bipolar signal (i.e. bipolar signals were obtained from electrode contact pairs located next to each other on the same electrode shaft). From all of the white – gray location combinations across patients ($n=202$), 71 showed significant link between gray and white matter signal for the 'passive watching' state ('sleep': 64 over $n=204$; 'active discussion': 76 over $n=212$). The results are depicted in Fig. 7 part A where each circle – either open or filled – represented a significant signal correlation between a white matter location and a gray matter location, the abscissa being the corresponding distance between the two locations (see Supplementary Fig. 7 for 'sleep' and 'active discussion' states). Although the signal recorded locally in the white matter was of smaller amplitude (see Fig. 7 part B), it was correlated with gray matter activity originating centimeters away. This result raises the possibility that electrode contacts located in the white matter recorded neuronal activity traveling along axonal tracts between distant cortical sites.

To determine whether distant white-gray matter signal correlations could be better explained by a gray matter source adjacent to the white matter, we examined the relationship between the signal from nearby gray matter and the sites showing distant white-gray matter signal correlations. For each white matter contact pair showing significant correlation with a distant cortical site, we identified the closest - termed the "adjacent" - gray matter contact. We next calculated the correlation of signals between the "adjacent" gray matter contact (referenced locally) and the local white matter contact pair, and between the “adjacent” gray matter

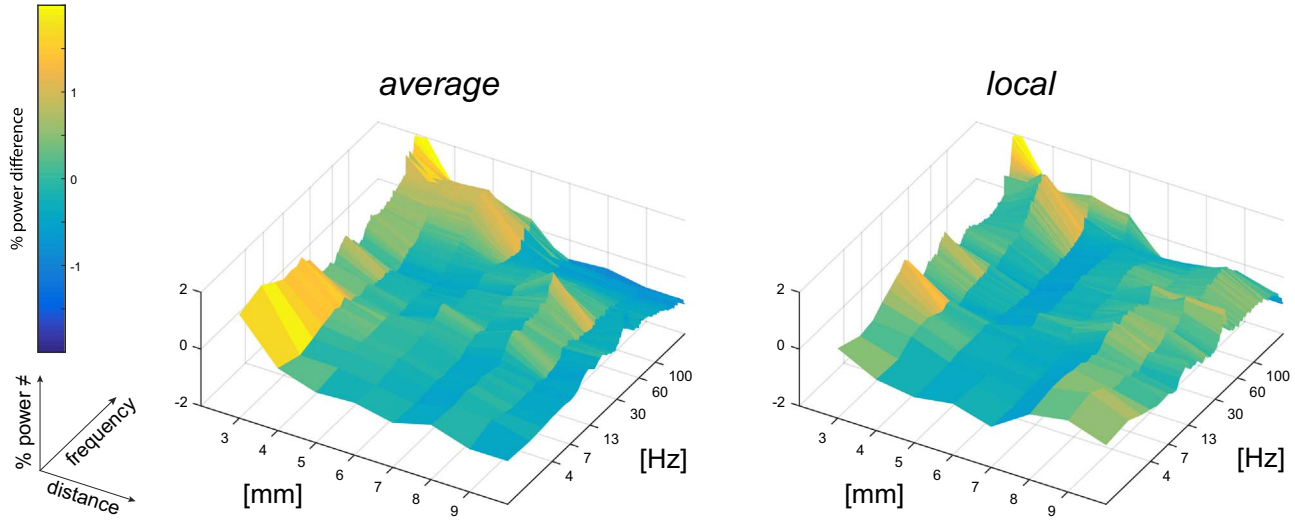

Fig. 6. Influence of passive spread on Power Spectra Density, Relative difference between the PSD corresponding to different distances (in mm) to the gray matter for electrodes fully surrounded by white matter (PTD$=-1$) and the mean PSD (across distance bin means). Results are presented for the average and the local reference montage. Relative power difference is represented on the *z*-axis and using the color code. Frequencies are depicted using a log scale. Data correspond to the 'passive watching' state.

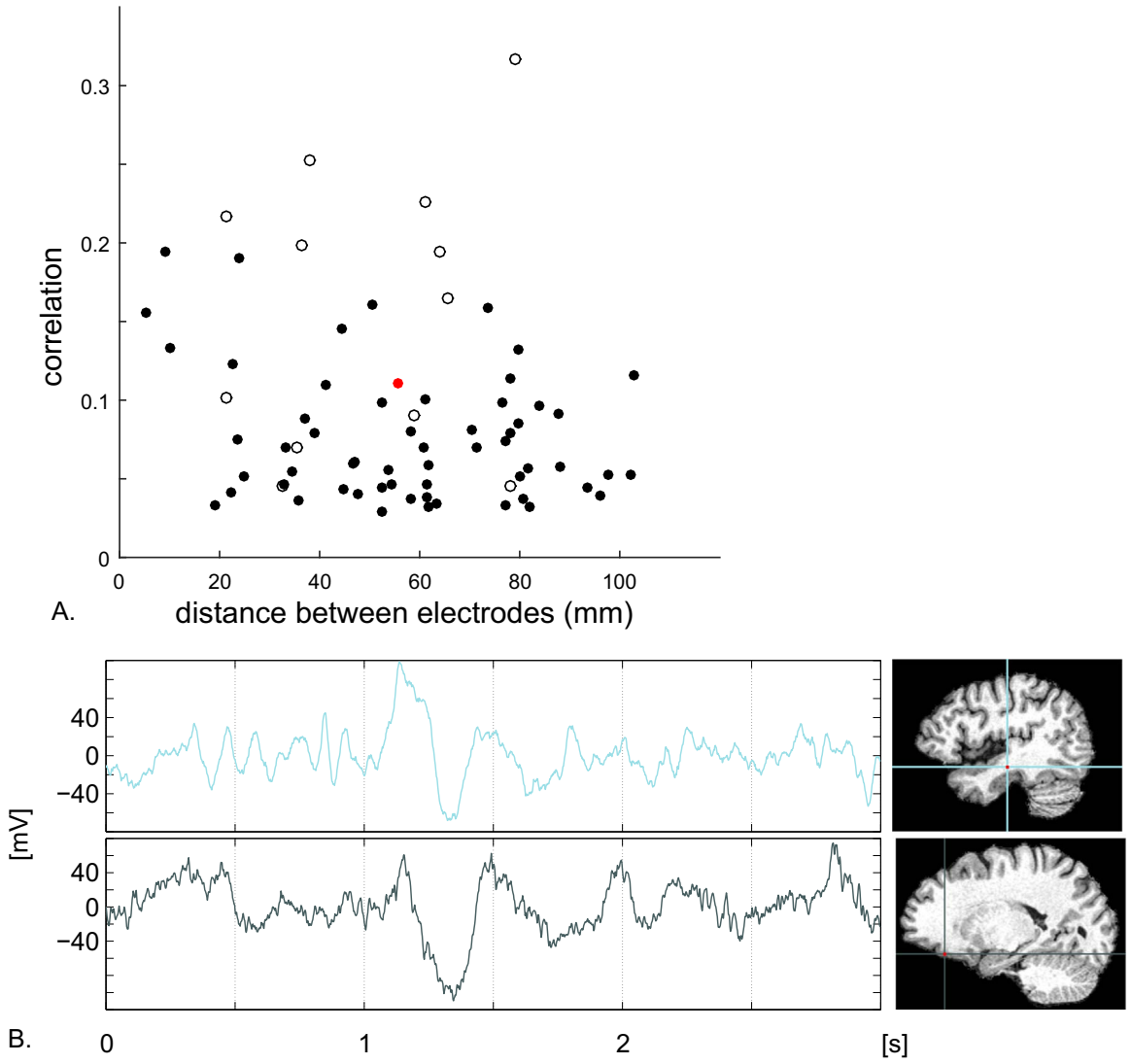

Fig. 7. Correlation between local white matter and local gray matter activity, **A.** Mean correlation between signals from electrodes located entirely in the white matter and electrodes located entirely in the gray matter plotted against the distance between them. Empty/filled circles represent white-gray electrodes pairs that show respectively significant/not significant correlation with the closest adjacent gray matter electrode located near the white matter electrode. **B.** Example of two bipolar signals significantly correlated along time depicted by the red circle in A. (r=.43 for the 3 s period; light gray and dark gray correspond to white and gray matter). The location of the midpoint between the electrode contact pairs located in the white and gray matter are depicted in sagittal views of the patient brain. Data correspond to the 'passive watching' state.

contact (referenced locally) and the distant gray matter contact pair. "Adjacent" gray matter showing significant correlation with both sites could be a 'common driver' accounting for the correlation between the local white matter signal and distant gray matter signal. Of the 71 significant correlations between gray and white matter signal present in the 'passive watching' state, 12 were significantly correlated with a common gray matter source "adjacent" to the white matter (for 'sleep' state: 15 of n=62, and for 'active discussion' state: 22 of 79). The gray-white pairs showing significant correlation with each other and with an "adjacent" gray site are shown as open circles in Fig. 7 (for 'passive watching', see Supplementary Fig. 7 for other states), while gray-white pairs showing significant correlation with each other but not with an "adjacent" gray site are shown as filled circles. This last analysis revealed that long distance correlation may originate from common input from nearby gray matter in a minority instances (17% in the 'passive watching' state), and that those cases tended to show the strongest correlations most likely reflecting long range cortical connectivity. In the majority of instances of long distance correlation between local white and distant gray sites, however, no common driver in adjacent cortex was found.

3.5. Local and distant signal time delays

To examine how signal correlation may be influenced by montage reference and by passive spread, we computed the cross-correlation lags between white matter signal and "adjacent" gray matter signal using signals referenced to a global average reference and signals referenced locally (white bipolar reference for white matter signal and gray bipolar reference for gray matter signal as in 3.4). The corresponding lag distributions were compared using the two-sample Kolmogorov-Smirnov test which showed a significant difference for all brain state ('passive watching': p=0.03; 'sleep': $p < 0.001$; 'active discussion': $p < 0.05$). As it can be seen in Fig. 8 (for 'passive watching', for other states see Supplementary Figs. 8), the distribution of cross-correlation lags is narrowed with more frequent zero lags when signals were referenced to the average as compared to a local montage reference. This high amount of zero delay correlation, and reduced amount of extended time-lag, may likely be caused by the effect of passive spread that is characterized by zero time-delay. This difference might also be influenced by the common averaged signal shared between the two signals.

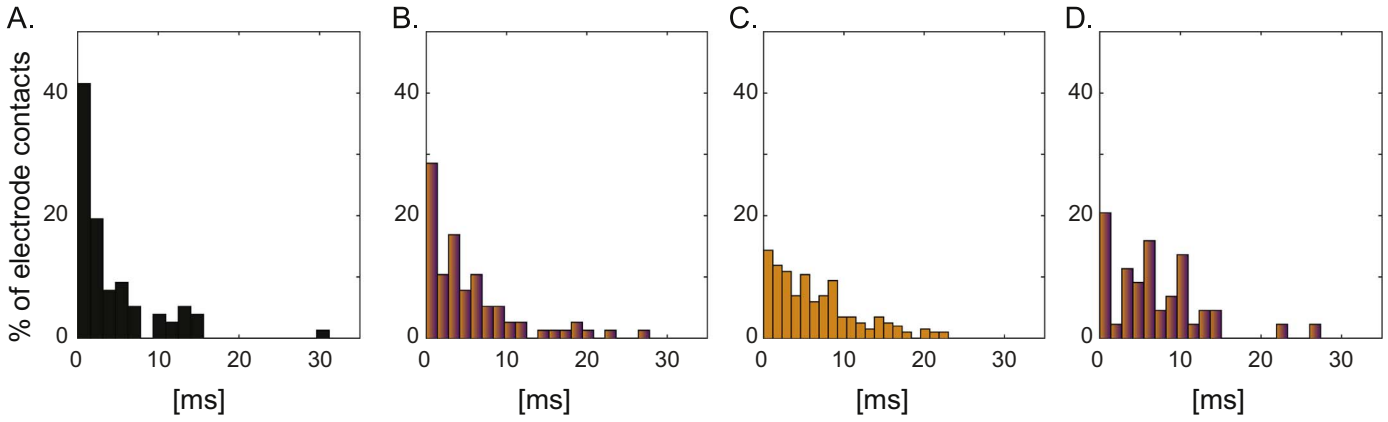

Fig. 8. Time lags distributions, Time lags distributions from cross-correlations computed between different signals. Abscissa represents time in milliseconds. Ordinate represents the proportion of electrode contacts in a given time-lag bin, with data organized in 20 different bins of time-lags along time dimension. The different time lags distributions correspond to: **A.** Cross-correlation ($n=77$) between white matter signal and signal of the closest gray matter electrode contact. Signal were referenced to an average reference (Mean=4.2, Mean Absolute Deviation=3.8), **B.** Cross-correlation ($n=77$) between bipolar white matter signal and bipolar signal of the closest gray matter electrode contacts. Signal were referenced to a local reference montage ($M=5.5$, MAD=4.3), **C.** Cross-correlation ($n=202$) between bipolar white matter signal and bipolar signal of distant electrode contact ($M=6.5$, MAD=4.2), **D.** Cross-correlation ($n=44$) between local signal of the closest gray matter electrode contact to the white matter electrodes contacts (as in B.) and bipolar signal of distant electrode contact ($M=7.0$, MAD=4.2). Colors of the bars indicate the reference montage used to compute the cross-correlations between the electrode contacts (same color code used in Fig. 5): Black for average reference, orange for bipolar, and purple for local reference montage.

The same analysis was performed to compare the lag distributions obtained from cross-correlation between the bipolar white matter signal and the "adjacent" local gray matter signal against two other lags distribution: from the cross-correlation between the local white matter signal and the distant bipolar gray matter and the "adjacent" local gray matter signal. The Kolmogorov–Smirnov tests were significant only for 'passive watching' state (respectively $p=0.03$ and $p=0.04$; for other states all p-values >0.4). As it can be seen in Fig. 8 and Supplementary Fig. 8, the lags distributions tend to be similar across computed cross-correlations. In other words, the distance between the signals considered for the cross-correlation, as well as the tissue type (i.e. white or gray matter) do not lead to different patterns of time lag distribution.

4. Discussion

In the present S-EEG study, we first examined the influence of different reference montages in common use (subdermal, white matter average, overall average and local) on signal correlation. As most reference montages include signals recorded in the white matter, we aimed at investigating the differences between that white matter signal and the signal recorded in the gray matter. Our analyses revealed that gray matter activity generally shows higher absolute amplitude compared to white matter, and that gray matter signal spreads passively (with zero time delay) into white matter. In addition to this signal spread, electrode contacts located in the white matter record low amplitude activity seemingly from the white matter fiber tracts themselves. In order to isolate this local white matter signal, the analysis must take into account tissue surrounding electrode contacts (e.g. using PTD) and must use a reference montage that avoids mixing signals to best discard contamination by volume conduction from nearby gray matter (Bastos and Schoffelen, 2015; Kajikawa and Schroeder, 2011, 2015). Our findings underscore the complexity attached to even the use of the term “local field potential”, as it implies that the signal originates very close to the active electrode, when in most cases, it does not. Also our results raise questions about the physiological origin of field potentials recorded in the white matter using S-EEG – the correlation of white matter signal with even distant cortical regions at non-zero time lag- and underscore the importance of considering the anatomical origin of signals when analyzing S-EEG data.

4.1. The different reference montages

Re-referencing the signal from human S-EEG recordings must be considered carefully as the reference can add noise, artifacts and/or passively spread activity to the recorded data, leading to spurious signal correlations that adversely impact S-EEG spatial resolution and can confound S-EEG analyses (see (Kovach et al., 2011) for an example of EMG contamination). In this section we describe the different commonly used reference montages and detail how our findings illustrate their inherent drawbacks.

A subdermal reference is generally used for intracranial recording as it has advantages in practicality and signal quality over a skull screw or surface disc electrode (Vulliemoz et al., 2010). However, the subdermal reference adds electrical brain activity recorded at the scalp to intracranial recordings and consequently reduces sensitivity and spatial resolution by increasing positive correlation between electrode contacts (see Fig. 2 and Supplementary Fig. 1 and 2, and (Zaveri et al., 2000)).

The rationale behind the average reference assumes that on average (1) the uncorrelated signals recorded from all electrode contacts cancel out when summed, resulting in a "random" signal of negligible amplitude, while (2) common signal to all intracranial electrode contacts sums constructively and is then removed when the average signal is subtracted from each electrode's signal (Boatman-Reich et al., 2010; Sinai et al., 2009). However, the average reference may either introduce or reveal additional negative correlations between channels (see Fig. 3 and Supplementary Fig. 3). Whether such negative correlations are meaningful is unclear, and echoes an ongoing debate in functional neuroimaging, where the interpretations of BOLD negative correlations have been challenged. Analogous to the average reference, global signal regression is a commonly used pre-processing step in the analysis of resting functional MRI data, which subtracts the common fluctuation of BOLD signal across all image voxels. The resulting negative correlations may be interpreted as revealing physiologically significant relationships (Fox et al., 2009; Keller et al., 2013), or may be interpreted as introducing spurious anti-correlations (Murphy et al., 2009; Weissenbacher et al., 2009).

Local referencing creates a second spatial derivative signal

(Hjorth, 1975; Mitzdorf, 1985; Perrin et al., 1987), which emphasizes local signal variations by subtracting the activity of neighboring electrode contacts. The use of the local reference removes signal that is common between the nearby *active* electrode and *reference* electrode(s), so that the remaining signal better reflects the activity unique to the *active* electrode. Consequently, this local montage increases spatial resolution and sensitivity by reducing signal correlation between electrodes (Bastos and Schoffelen, 2015; Mercier et al., 2015; Shirhatti et al., 2016), which is essential for functional connectivity analysis (so long as the connectivity measure is computed between non-adjacent electrodes, since adjacent electrodes will be artificially correlated).

Yet another approach to referencing S-EEG signals treats electrode contacts located in the white matter as neutral, and uses these electrode(s) as reference(s). However, our results indicate that this approach can introduce a larger bias than the average reference or the local montage as measured by inter-electrode correlation. As it can be seen in Fig. 2 and Supplementary Fig. 1 and 2, the contribution of signal recorded in the white matter (PTD$=-1$) to common signal through the reference is non-negligible, and even larger than the one introduced by the use of a reference average of gray matter electrode contacts (PTD$=1$), raising questions about the physiological origin of local white matter signal. In the next section, after discussing the differences between signals recorded from white and gray matter, we present two non-exclusive explanations for the origin of white matter signal: first by demonstrating that electrode contacts located in the white matter record signal spread passively from adjacent gray matter; and second, by showing that the signal recorded in the white matter is correlated with signals from distant gray matter presumably propagated through white matter tracts if not by a common driver in the gray matter nearby the white matter.

4.2. White matter signal versus gray matter activity

The S-EEG field potential has been attributed to post-synaptic potentials localized in cortical gray matter (Lachaux et al., 2012, 2003), as opposed to action potentials, the primary type of neural activity ascribed to white matter. The different mechanisms giving rise to the S-EEG signal can be inferred from the difference between gray and white matter architectonics. The shared dipolar orientation of pyramidal cell apical dendrites and the relatively long monophasic duration (>15 ms) of synaptic currents allows volume integration and temporal summation of local synchronous synaptic currents into large extracellular potential fields that can be detected by macro-electrodes (see Kajikawa and Schroeder, 2015 for an in-depth analysis of this issue). In contrast, white matter voltages arise from short duration ($\sim$1 ms) action potentials with a quadrupolar extracellular field, resulting in greater destructive spatial and temporal interference, and hence attenuation, in the summation of action potentials into a macroscopic potential. What is more, gray matter and white matter have different electrical conductivity as a result of the presence of myelin that acts as an insulator and reduces the spread of electric potentials, with impedance in white matter ranging between 800 to 1000 Ω, compared to 500–700 Ω in gray matter (Lozano et al., 2009). Based on these expected differences, we investigated if there were differences in spectral power or absolute signal amplitude between signals recorded in both tissues. Overall, our results show greater power and larger fluctuations in the mean amplitude of activity from electrode contacts located in the cortical gray matter compared to contacts in white mater. However, as it can be seen in Fig. 4 part B, it is not possible to consistently distinguish whether single electrode contacts belong to gray or white matter based solely on the characteristics of electrical activity at that location (see also Supplementary Fig. 4). Indeed some electrode contacts located in the white matter can present signal characteristics similar to the ones located in the gray matter and vice and versa. This observation suggests further that white matter signal, as recorded with stereotactic electrodes, cannot be entirely discounted as negligible.

In a series of analyses, we aimed at investigating the possible origins of the white matter signal. First, we assessed signal passive spread from gray matter to white matter. Our results show that the absolute signal amplitude of white matter signal is inversely correlated with the distance to gray matter (Fig. 5 and Supplementary Fig. 5). This is not the case when the signal is referenced locally, either by using a local reference, or by applying a bipolar reference on contiguous electrode contacts of the same shaft (both located in the white matter). That is to say, when the signal is spatially focused, by removing common signal from neighboring electrode contacts, the absolute signal amplitude is independent of the distance to the gray matter. This result suggests that the high amplitude fluctuations from the gray matter spread by volume conduction to electrode contacts located in the white matter. Moreover the passive spread is also visible in the profile of the power spectra signal from white matter electrode contacts. And, power content across frequencies follows a u-shape distribution with distance (Fig. 6 and Supplementary Fig. 6). These findings suggest that in white matter part of the broad band power arises from passive spread of activity from gray matter, while another part may originate locally and not from nearby gray matter.

Importantly, we observed that the white matter signal can be correlated with gray matter activity located several centimeters away. Yet, it could be that the long distance correlations measured between bipolar white matter signal and local gray matter signals were due to residual volume conduction. In this scenario, there could be correlated activity between distantly separated gray matter regions, and then passive spread of signal from nearby gray matter, the 'common driver', would create the appearance that white matter is correlated with the distant gray matter signal. The last series of analysis show that only a small portion ($\sim$17%) of the correlated white-gray matter signals can be explained by residual volume conduction from nearby gray matter that is itself significantly correlated with distant gray matter. However, the proximal gray matter signal was only partially sampled spatially in the vicinity of the white matter electrode contacts. Fully assessing whether the signals obtained after re-referencing entirely cancel out all local gray matter activity would require a 3D spatial sampling surrounding each white matter locus, which is regrettably technically not possible here.

Based on examination of cross-correlation, we also estimated the distribution of cross-correlation time lags between different signals. Initial analysis showed a larger cross-correlation zero time lags between white matter signal and nearby gray matter signal when an average reference signal is used as compared to local reference montage. This result illustrates the characteristic zero time delay associated with passive spread, but may be influenced by the shared signal introduced by the average reference montage. Next, the same analysis of the distribution of cross-correlation time lags was performed between bipolar signals recorded in the white matter, nearby gray matter and distant gray matter. In all cases the time lag distributions ranged between 0 to 20 ms, with similar time lags distribution patterns between the different cross-correlated signals, suggesting a different mechanism than passive diffusion.

The signal recorded from white matter tracts can also reflect neuronal communication between distant regions of cortex through white matter fiber tracts. While our results of time lag distribution analysis have to be cautiously interpreted, they may illustrate rapid transmission with short delays (cross brain conduction time has been reported as low as 5 ms in humans (Wang

et al., 2008)). This finding challenges the generally held idea that white matter does not contribute significantly to the field potential because of destructive interference between positive and negative phases of the action potentials and because of the quadrapolar field created by it. The origin of the white matter signal is for the most part unclear. In some well-studied cases, such as brainstem auditory evoked potentials (BAEP), white matter action potentials can be detected at great distances. In this example, the action potential discharge is triggered by a brief auditory click. The BAEP activity, however, differs importantly from cerebral white matter activity in that BAEP activity is tightly localized to the brainstem auditory pathways, and the action potentials giving rise to the BAEP are time-locked to the auditory stimulus, minimizing destructive spatial or temporal interference (Legatt et al., 1988). White matter activity in the forebrain is neither well localized, as axonal branching may direct activity into multiple tracts, nor temporally synchronized, as the activity in adjacent tracts may arise from unrelated sources. The brief duration of action potentials would be expected to largely – but not entirely – cancel out when the activity of multiple axons is summed. However, the power spectral profile of summed action potentials might be expected to preserve a similar spectral profile as individual action potentials (i.e. high frequencies), which is not the case in our data. Our data show that the spectral power profile of white matter is similar, though lower in magnitude, to that of gray matter. Indeed, white matter signal power at the lowest frequencies is significantly greater than the spectral power at higher frequencies more typical of action potentials. Several mechanisms may contribute to low frequency activity in white matter. The extracellular action potential may not be entirely biphasic inasmuch as extracellular concentration of potassium increases during a burst of action potentials, causing a shift in resting membrane potential. The net movement of axonal membrane potential from initial resting potential to final resting potential represents the effect of net non-zero low-frequency current flow, which when summated across axons may interact constructively (Gulledge et al., 2013; Thompson and Prince, 1986). A related interpretation is that the summated white matter local field potential reflects the temporal envelope of trains of action potential. Further, the restoration of electrochemical gradients of sodium, potassium, and possibly calcium (Dreier and Reiffurth, 2015) that have declined after sustained axonal activity requires the action of the electrogenic sodium-potassium ATPase that expels 3 sodium ions for every two potassium ions that enter (Krishnan et al., 2015). We can also speculate that the induction of sodium potassium ATPase activity in response to increased white matter activity could result in coupling of high frequency firing of action potentials to low frequency changes in local field potential, and may correspond to the white matter BOLD changes reported in some fMRI studies (see review by (Gawryluk et al., 2014), and (Mazerolle et al., 2008, 2013) as examples).

Additionally, we cannot exclude the contribution of a common drive as might result from the action of a neuromodulatory system. Neuromodulatory systems can regulate activity in a large population of neurons and are furthermore closely linked to the glia that form an intricate network with the neurons (Auld and Robitaille, 2003; Bezzi and Volterra, 2001). Glia under the influence of neuromodulatory input may in turn influence local activity and regulate neuronal communication by altering local electrolyte gradients, and may even influence behavioral states such as motivation, wakefulness or sleep (Laming, 1989; Laming et al., 2000). Therefore, in the present case, it could be hypothesized that a neuromodulatory system modulates both distant gray matter and local white matter, introducing correlation between the two.

4.3. Consequences for intracranial recordings

In the present study we introduced an alternative gradual approach to the generally used binary classification of the electrode contacts for two reasons. First, the procedure for co-registration and localization of electrode contacts on the MRI inherently requires several spatial approximations (see detailed explanation in the material and method section). Second, as we have shown, an electrode contact located in a given tissue records activity that spreads from other tissue located in proximity. We therefore defined a Proximal Tissue Density index (PTD), which takes into account the mix of gray and white matter surrounding the electrode contact and takes into account the approximation regarding electrode contact location. Comparison between a strict binary (i.e. only based on centroid location: either gray or white matter) and the present gradual method to classify electrode contacts revealed that for only 40% of electrode contacts the surrounding tissue was entirely of one type only (i.e. a PTD value of -1 or 1). A majority of electrode contacts were surrounded to a varying degree, by a mix of tissues, which reveal the importance of considering tissue composition surrounding the electrode contact centroid.

In a recent publication, Arnulfo and colleagues introduced an index named Gray Matter Proximity Index (GMPI), calculated for each electrode, and corresponding to the distance to the nearest white-matter interface, normalized by cortical thickness (Arnulfo et al., 2015). They used this GMPI index to categorize electrode contacts that belong either to the gray or to the white matter, and further proposed to re-reference each gray matter electrode contact to the nearest white matter electrode contact. While we confirmed their presumption regarding the passive spread of electrical fields generated in the gray matter to the nearby white matter (up to 4–5 mm), our results also show that white matter contacts cannot be considered entirely as a 'neutral reference', as these electrode contacts record (i) activity that spread from nearby surrounding gray matter (which could correspond to a different functional area or cortex), and potentially (ii) activity traveling along the fiber tracts from remote cortical regions. As a consequence it appears that there is no perfect reference montage scheme, but rather different options, each with unique advantages and limitations.

These issues are critical for the clinicians as well as for the researchers. For the epileptologists, neurologists, or neurosurgeons, it is essential to know whether epileptic activity is emanating from tissue located immediately surrounding an electrode contact or from activity either diffused from neighboring cortical regions or trafficked along white matter connections of an epileptical network (Yaffe et al., 2014). For the researcher, who wants to investigate the signals associated with experimental manipulations, the same question arises: is the measured activity originating locally or remotely? We propose that two reference montages should be compared to assess the spatial resolution of a given observation ; especially including the local montage reference (see description in Section 2.4) or the proximal white matter scheme (as defined in (Arnulfo et al., 2015)). As shown in our data, the local reference montage greatly improves spatial resolution by reducing volume conduction. Also the use of the local environment around each electrode contact is definitely helping to ascertain the degree of confidence that the source of the recorded activity originated locally.

5. Conclusion

In the present study we examined the influence of the reference choice on S-EEG signal and considered the influence of passive signal spread from the gray matter. Since commonly used

reference montages include electrode contacts not only located in cortical gray matter, but also in white matter fibers, we aimed at investigating if the signals recorded in those tissues have different characteristics. We explored this question using a gradual classification approach allowing us to consider electrode contact localization uncertainty. Our results suggest that the signal recorded by electrode contacts located in the white matter contains a mixture of signals spread passively from nearby gray matter as well as smaller amplitude signal that could, in some cases, correlate to neuronal activity from distant gray matter. We considered different mechanisms that could account for this long distance white-gray matter correlation along with the hypothesis that white matter signal may reflect neuronal activity propagating along axonal tracts. These findings highlight three important challenges inherent in analyzing S-EEG, namely understanding (i) the consequences of mixing the signals from the reference and recording electrodes, (ii) the importance of considering surrounding tissue in determining electrode contact 3D location, (iii) the influence of volume conduction on locally recorded local field potentials.

Acknowledgments

Part of the data analysis was performed using the Fieldtrip toolbox for EEG/MEG-analysis, developed at the Donders Institute for Brain, Cognition and Behavior (Oostenveld et al., 2011), and the Mass Univariate ERP Toolbox. *OpenWetWare* (Groppe et al., 2011a, 2011b).

We wish to thank J. Matias Palva for helpful comments on an earlier version of the manuscript, and Dr. Solomon Moshé for his support of this work.

The authors declare no competing financial interests that would bias the results reported here.

Appendix A. Supplementary material

Supplementary data associated with this article can be found in the online version at http://dx.doi.org/10.1016/j.neuroimage.2016.08.037.

References

Arnulfo, G., Hirvonen, J., Nobili, L., Palva, S., Palva, J.M., 2015. Phase and amplitude correlations in resting-state activity in human stereotactical EEG recordings. NeuroImage 112, 114–127.
Auld, D.S., Robitaille, R., 2003. Glial cells and neurotransmission: an inclusive view of synaptic function. Neuron 40, 389–400.
Bancaud, J., Talairach, J., 1973. Methodology of stereo EEG exploration and surgical intervention in epilepsy. Rev. Otoneuroophtalmol. 45, 315–328.
Bastos, A.M., Schoffelen, J.M., 2015. A tutorial review of functional connectivity analysis methods and their interpretational pitfalls. Front. Syst. Neurosci. 9, 175.
Bezzi, P., Volterra, A., 2001. A neuron-glia signalling network in the active brain. Curr. Opin. Neurobiol. 11, 387–394.
Benjamini, Y., Yekutieli, D., 2001. The control of the false discovery rate in multiple testing under dependency. The Annals of Statistics 29 (4), 1165–1188.
Boatman-Reich, D., Franaszczuk, P.J., Korzeniewska, A., Caffo, B., Ritzl, E.K., Colwell, S., Crone, N.E., 2010. Quantifying auditory event-related responses in multichannel human intracranial recordings. Front. Comput. Neurosci. 4, 4.
Butler, J.S., Molholm, S., Fiebelkorn, I.C., Mercier, M.R., Schwartz, T.H., Foxe, J.J., 2011. Common or redundant neural circuits for duration processing across audition and touch. J. Neurosci. 31, 3400–3406.
Dalal, S.S., Edwards, E., Kirsch, H.E., Barbaro, N.M., Knight, R.T., Nagarajan, S.S., 2008. Localization of neurosurgically implanted electrodes via photograph-MRI-radiograph coregistration. J. Neurosci. Methods 174, 106–115.
Destrieux, C., Fischl, B., Dale, A., Halgren, E., 2010. Automatic parcellation of human cortical gyri and sulci using standard anatomical nomenclature. NeuroImage 53, 1–15.
Dreier, J.P., Reiffurth, C., 2015. The stroke-migraine depolarization continuum. Neuron 86, 902–922.
Dykstra, A.R., Chan, A.M., Quinn, B.T., Zepeda, R., Keller, C.J., Cormier, J., Madsen, J.R., Eskandar, E.N., Cash, S.S., 2012. Individualized localization and cortical surface-based registration of intracranial electrodes. NeuroImage 59, 3563–3570.
Fischl, B., van der Kouwe, A., Destrieux, C., Halgren, E., Segonne, F., Salat, D.H., Busa, E., Seidman, L.J., Goldstein, J., Kennedy, D., Caviness, V., Makris, N., Rosen, B., Dale, A.M., 2004. Automatically parcellating the human cerebral cortex. Cereb. Cortex 14, 11–22.
Fox, M.D., Zhang, D., Snyder, A.Z., Raichle, M.E., 2009. The global signal and observed anticorrelated resting state brain networks. J. Neurophysiol. 101, 3270–3283.
Gawryluk, J.R., Mazerolle, E.L., Beyea, S.D., D'Arcy, R.C., 2014. Functional MRI activation in white matter during the symbol digit modalities test. Front. Hum. Neurosci. 8, 589.
Gomez-Ramirez, M., Kelly, S.P., Molholm, S., Sehatpour, P., Schwartz, T.H., Foxe, J.J., 2011. Oscillatory sensory selection mechanisms during intersensory attention to rhythmic auditory and visual inputs: a human electrocorticographic investigation. J. Neurosci. 31, 18556–18567.
Groppe, D.M., Urbach, T.P., Kutas, M., 2011a. Mass univariate analysis of event-related brain potentials/fields I: a critical tutorial review. Psychophysiology 48, 1711–1725.
Groppe, D.M., Urbach, T.P., Kutas, M., 2011b. Mass univariate analysis of event-related brain potentials/fields II: Simulation studies. Psychophysiology 48, 1726–1737.
Groppe, D.M., Bickel, S., Keller, C.J., Jain, S.K., Hwang, S.T., Harden, C., Mehta, A.D., 2013. Dominant frequencies of resting human brain activity as measured by the electrocorticogram. NeuroImage 79, 223–233.
Gulledge, A.T., Dasari, S., Onoue, K., Stephens, E.K., Hasse, J.M., Avesar, D., 2013. A sodium-pump-mediated after hyperpolarization in pyramidal neurons. J. Neurosci. 33, 13025–13041.
Hermes, D., Miller, K.J., Noordmans, H.J., Vansteensel, M.J., Ramsey, N.F., 2010. Automated electrocorticographic electrode localization on individually rendered brain surfaces. J. Neurosci. Methods 185, 293–298.
< http://biorxiv.org/content/early/2016/08/11/069179 > .
Hjorth, B., 1975. An on-line transformation of EEG scalp potentials into orthogonal source derivations. Electroencephalogr. Clin. Neurophysiol. 39, 526–530.
Jenkinson, M., Smith, S., 2001. A global optimisation method for robust affine registration of brain images. Med. Image Anal. 5, 143–156.
Kajikawa, Y., Schroeder, C.E., 2011. How local is the local field potential? Neuron 72, 847–858.
Kajikawa, Y., Schroeder, C.E., 2015. Generation of field potentials and modulation of their dynamics through volume integration of cortical activity. J. Neurophysiol. 113, 339–351.
Keller, C.J., Honey, C.J., Entz, L., Bickel, S., Groppe, D.M., Toth, E., Ulbert, I., Lado, F.A., Mehta, A.D., 2014. Corticocortical evoked potentials reveal projectors and integrators in human brain networks. J. Neurosci. 34, 9152–9163.
Keller, C.J., Bickel, S., Honey, C.J., Groppe, D.M., Entz, L., Craddock, R.C., Lado, F.A., Kelly, C., Milham, M., Mehta, A.D., 2013. Neurophysiological investigation of spontaneous correlated and anticorrelated fluctuations of the BOLD signal. J. Neurosci. 33, 6333–6342.
Ken, S., Di Gennaro, G., Giulietti, G., Sebastiano, F., De Carli, D., Garreffa, G., Colonnese, C., Passariello, R., Lotterie, J.A., Maraviglia, B., 2007. Quantitative evaluation for brain CT/MRI coregistration based on maximization of mutual information in patients with focal epilepsy investigated with subdural electrodes. Magn. Reson. Imaging 25, 883–888.
Kovach, C.K., Tsuchiya, N., Kawasaki, H., Oya, H., Howard 3rd, M.A., Adolphs, R., 2011. Manifestation of ocular-muscle EMG contamination in human intracranial recordings. NeuroImage 54, 213–233.
Krishnan, G.P., Filatov, G., Shilnikov, A., Bazhenov, M., 2015. Electrogenic properties of the Na+/K+ ATPase control transitions between normal and pathological brain states. J. Neurophysiol. 113, 3356–3374.
Kutas, M., Dale, A., 1997. Electrical and magnetic readings of mental functions. Cogn. Neurosci., 1974242.
Lachaux, J.P., Rudrauf, D., Kahane, P., 2003. Intracranial EEG and human brain mapping. J. Physiol. Paris 97, 613–628.
Lachaux, J.P., Axmacher, N., Mormann, F., Halgren, E., Crone, N.E., 2012. High-frequency neural activity and human cognition: past, present and possible future of intracranial EEG research. Prog. Neurobiol. 98, 279–301.
Laming, P.R., 1989. Do glia contribute to behaviour? A neuromodulatory review. Comp. Biochem. Physiol. A Comp. Physiol. 94, 555–568.
Laming, P.R., Kimelberg, H., Robinson, S., Salm, A., Hawrylak, N., Muller, C., Roots, B., Ng, K., 2000. Neuronal-glial interactions and behaviour. Neurosci. Biobehav. Rev. 24, 295–340.
LaViolette, P.S., Rand, S.D., Ellingson, B.M., Raghavan, M., Lew, S.M., Schmainda, K. M., Mueller, W., 2011. 3D visualization of subdural electrode shift as measured at craniotomy reopening. Epilepsy Res. 94, 102–109.
Legatt, A.D., Arezzo, J.C., Vaughan Jr., H.G., 1988. The anatomic and physiologic bases of brain stem auditory evoked potentials. Neurol. Clin. 6, 681–704.
Lozano, A.M., Gildenberg, P.L., Tasker, R.R., 2009. Textbook of Stereotactic and Functional Neurosurgery, 2d ed Springer, Verlag Berlin Heidelberg.
Mazerolle, E.L., D'Arcy, R.C., Beyea, S.D., 2008. Detecting functional magnetic resonance imaging activation in white matter: interhemispheric transfer across the corpus callosum. BMC Neurosci. 9, 84.
Mazerolle, E.L., Gawryluk, J.R., Dillen, K.N., Patterson, S.A., Feindel, K.W., Beyea, S.D., Stevens, M.T., Newman, A.J., Schmidt, M.H., D'Arcy, R.C., 2013. Sensitivity to white matter FMRI activation increases with field strength. PLoS One 8, e58130.
Mercier, M.R., Foxe, J.J., Fiebelkorn, I.C., Butler, J.S., Schwartz, T.H., Molholm, S., 2013.

Auditory-driven phase reset in visual cortex: human electrocorticography reveals mechanisms of early multisensory integration. NeuroImage 79, 19–29.
Mercier, M.R., Molholm, S., Fiebelkorn, I.C., Butler, J.S., Schwartz, T.H., Foxe, J.J., 2015. Neuro-oscillatory phase alignment drives speeded multisensory response times: an electro-corticographic investigation. J. Neurosci. 35, 8546–8557.
Miller, K.J., Makeig, S., Hebb, A.O., Rao, R.P., denNijs, M., Ojemann, J.G., 2007. Cortical electrode localization from X-rays and simple mapping for electrocorticographic research: the "Location on Cortex" (LOC) package for MATLAB. J. Neurosci. Methods 162, 303–308.
Mitzdorf, U., 1985. Current source-density method and application in cat cerebral cortex: investigation of evoked potentials and EEG phenomena. Physiol. Rev. 65, 37–100.
Murphy, K., Birn, R.M., Handwerker, D.A., Jones, T.B., Bandettini, P.A., 2009. The impact of global signal regression on resting state correlations: are anti-correlated networks introduced? NeuroImage 44, 893–905.
Oostenveld, R., Fries, P., Maris, E., Schoffelen, J.M., 2011. FieldTrip: Open source software for advanced analysis of MEG, EEG, and invasive electrophysiological data. Comput. Intell. Neurosci. 2011, 156869.
Penfield, W., Steelman, H., 1947. The treatment of focal epilepsy by cortical excision. Ann. Surg. 126, 740–761.
Perrin, F., Bertrand, O., Pernier, J., 1987. Scalp current density mapping: value and estimation from potential data. IEEE Trans. Biomed. Eng. 34, 283–288.
Sebastiano, F., Di Gennaro, G., Esposito, V., Picardi, A., Morace, R., Sparano, A., Mascia, A., Colonnese, C., Cantore, G., Quarato, P.P., 2006. A rapid and reliable procedure to localize subdural electrodes in presurgical evaluation of patients with drug-resistant focal epilepsy. Clin. Neurophysiol. 117, 341–347.
Shepard, D., 1968. A two-dimensional interpolation function for irregularly-spaced data, In: Proceedings of the 23rd National Conference, ACM, pp. 517–524.
Shirhatti, V., Borthakur, A., Ray, S., 2016. Effect of reference scheme on power and phase of the local field potential. Neural Comput. 28, 882–913.
Sinai, A., Crone, N.E., Wied, H.M., Franaszczuk, P.J., Miglioretti, D., Boatman-Reich, D., 2009. Intracranial mapping of auditory perception: event-related responses and electrocortical stimulation. Clin. Neurophysiol. 120, 140–149.
Spiegel, E.A., Wycis, H.T., Marks, M., Lee, A.J., 1947. Stereotaxic apparatus for operations on the human brain. Science 106, 349–350.
Talairach, J., Szikla, G., 1980. Application of stereotactic concepts to the surgery of epilepsy. Acta Neurochir Suppl. 30, 35–54.
Talairach, J., Bancaud, J., Szikla, G., Bonis, A., Geier, S., Vedrenne, C., 1974. New approach to the neurosurgery of epilepsy. Stereotaxic methodology and therapeutic results. 1. Introduction and history. Neurochirurgie 20 (Suppl. 1), 1–240.
Thompson, S.M., Prince, D.A., 1986. Activation of electrogenic sodium pump in hippocampal CA1 neurons following glutamate-induced depolarization. J. Neurophysiol. 56, 507–522.
Vulliemoz, S., Spinelli, L., Pellise, D., Seeck, M., Ives, J.R., 2010. A new ground and reference technique for invasive EEG recordings. Am. J. Electroneurodiagnostic Technol. 50, 50–58.
Wang, S.S., Shultz, J.R., Burish, M.J., Harrison, K.H., Hof, P.R., Towns, L.C., Wagers, M. W., Wyatt, K.D., 2008. Functional trade-offs in white matter axonal scaling. J. Neurosci. 28, 4047–4056.
Weissenbacher, A., Kasess, C., Gerstl, F., Lanzenberger, R., Moser, E., Windischberger, C., 2009. Correlations and anticorrelations in resting-state functional connectivity MRI: a quantitative comparison of preprocessing strategies. NeuroImage 47, 1408–1416.
Yaffe, R.B., Borger, P., Megevand, P., Groppe, D.M., Kramer, M.A., Chu, C.J., Santaniello, S., Meisel, C., Mehta, A.D., Sarma, S.V., 2014. Physiology of functional and effective networks in epilepsy. Clin. Neurophysiol.
Zaveri, H.P., Duckrow, R.B., Spencer, S.S., 2000. The effect of a scalp reference signal on coherence measurements of intracranial electroencephalograms. Clin. Neurophysiol. 111, 1293–1299.
Zaveri, H.P., Duckrow, R.B., Spencer, S.S., 2006. On the use of bipolar montages for time-series analysis of intracranial electroencephalograms. Clin. Neurophysiol. 117, 2102–2108.